Journal of Power Sources 195 (2010) 5996–6000

Contents lists available at ScienceDirect

Journal of Power Sources

journal homepage: www.elsevier.com/locate/jpowsour

Short communication

Microelectrode-based hydrogen peroxide detection during oxygen reduction at Pt disk electrode

Akira Kishi, Takuya Fukasawa, Minoru Umeda*

Department of Materials Science and Technology, Faculty of Engineering, Nagaoka University of Technology, Kamitomioka 1603-1, Nagaoka, Niigata 940-2188, Japan

ARTICLE INFO

Article history:
Received 30 September 2009
Received in revised form 27 October 2009
Accepted 29 October 2009
Available online 10 November 2009

Keywords:
Microelectrode
H_2O_2
Scanning electrochemical microscopy
Nafion-coated electrode
Diffusion layer thickness

ABSTRACT

We investigated the diffusion process of H_2O_2 generated during O_2 reduction at a Pt microdisk electrode used as a generator for scanning electrochemical microscopy (SECM). First, the amount of O_2 consumption and generated H_2O_2 at the Pt generator electrode are estimated using a detector electrode installed in the SECM. Based on the results, a large amount of O_2 consumption and generated H_2O_2 are detected at the center of each generator electrode. According to the measurement, the O_2 starvation and H_2O_2 detection currents can be defined. Subsequently, the O_2 starvation and H_2O_2 detection currents are measured by varying the generator size. As a result, these currents decrease with a decrease in the generator electrode size, however, the H_2O_2 diffusion process is changed for the generator diameter of less than 50 μm. Finally, the O_2 starvation and H_2O_2 detection measurements were conducted using a Nafion-coated Pt microdisk electrode. The amount of O_2 consumption is not suppressed, while the amount of generated H_2O_2 decreases with the Nafion layer prepared on the Pt electrode. This result indicates that the thickness of the H_2O_2 diffusion layer in the H_2SO_4 solution is dramatically diminished by coating the Nafion layer on the Pt generator.

1. Introduction

The oxygen reduction reaction (ORR) at the Pt cathode of a polymer electrolyte fuel cell (PEFC) plays an important role in the power generation [1,2]. The O_2 reduction at the Pt electrode generates a slight amount of H_2O_2 as a by-product [3–6]. The H_2O_2 generated by the oxygen reduction is reported to degrade the polymer electrolyte membrane [7–10] and the Pt-based electrocatalyst [11]. It is, therefore, necessary to prevent the H_2O_2 from diffusing to the electrolyte membrane as well as to suppress the amount of the generated H_2O_2. For this reason, it is worthwhile to investigate the detailed process of the H_2O_2 diffusion from the Pt electrode to the polymer electrolyte membrane. In this study, we focused on the diffusion process of the H_2O_2 by-product into the electrolyte membrane.

The rotating disk electrode (RDE) is one technique to investigate the oxygen reduction reaction mechanism [12–14]. This can predict its reaction pathway by estimating the number of electrons which participate in the ORR from the Koutecky–Levich plot [12–14]. However, the amount of the generated H_2O_2 by-product is not known by this method. Thus, it is necessary to measure the amount of the H_2O_2 by-product by another technique.

As for the other techniques, the rotating ring disk electrode (RRDE) [15–17] and channel flow double electrode (CFDE) [18–20] are utilized to detect the H_2O_2 by-product generated during the O_2 reduction. In these techniques, the H_2O_2 is generated at the generator electrode, and the H_2O_2 is carried toward the detector electrode by a forced convection. The amount of H_2O_2 is estimated from the magnitude of the oxidation current at the detector [15–19]. However, the generated H_2O_2 diffuses in the practical PEFC cell. Therefore, it is necessary to detect the H_2O_2 without a forced convection to properly understand the H_2O_2 diffusion process in the PEFC.

In addition, scanning electrochemical microscopy (SECM) can be a technique to adequately evaluate the H_2O_2 diffusion without any forced convection [21,22]. The H_2O_2 is generated during the O_2 reduction at the generator electrode of the SECM. The generated H_2O_2 then diffuses to the detector, and the magnitude of the generated H_2O_2 can be estimated by the oxidation current [21,22]. The amount of the generated H_2O_2 has been investigated in previous studies [21,22], however, the generated H_2O_2 diffusion phenomena in the electrolyte solution and electrolyte membrane have not been investigated. To accomplish this objective, we selected the SECM as an appropriate technique.

In this study, the amount of the H_2O_2 by-product at the Pt microdisk electrode is semiquantitatively measured by the SECM. Subsequently, the method of estimating the H_2O_2 diffusion layer thickness is established. Moreover, by changing the generator

* Corresponding author. Tel.: +81 258 47 9323; fax: +81 258 47 9323.
E-mail address: mumeda@vos.nagaokaut.ac.jp (M. Umeda).

0378-7753/$ – see front matter © 2009 Elsevier B.V. All rights reserved.
doi:10.1016/j.jpowsour.2009.10.082

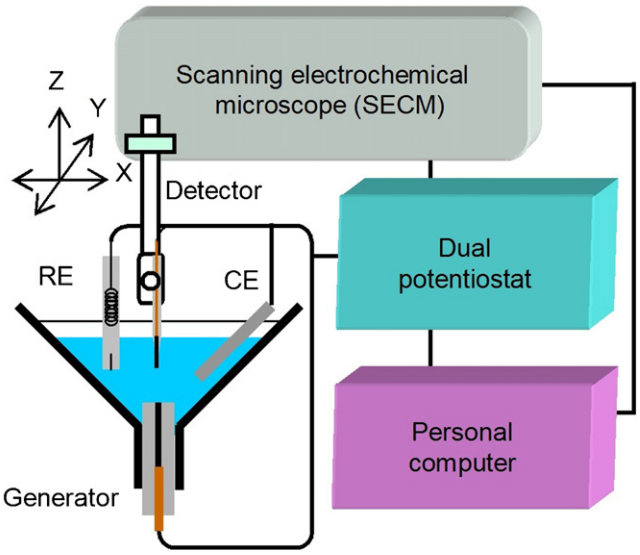

Fig. 1. Schematic of the scanning electrochemical microscopy setup.

diameter size, the amount and the diffusion layer thickness of the generated H_2O_2 were investigated. Finally, the Nafion-coated Pt microdisk electrode, which is a representative of the cathode catalyst layer of the PEFC, is used as the generator. As a result, the generated H_2O_2 is found to hardly pass through the Nafion layer.

2. Experimental

2.1. Preparation of electrodes

Pt microdisk electrodes used as a generator of the SECM were prepared as follows [23]. Pt wire of various diameters (20, 50, 100, 300 μm) was inserted inside the tip of the glass capillaries (ϕ 1.6 mm outer diameter). Subsequently, the tip of the capillary was heat-sealed. The tip was then polished using lapping films. The other type of the generator of the SECM, a Nafion-overcoated Pt microdisk electrode, was also prepared. A Nafion coating layer was prepared by dip coating a 5 wt.% Nafion solution (ion exchange capacity; 0.476 mmol g^{-1}, Wako Pure Chemical) using a dip coater (VLST-45-06-0100, Aiden) on the above-mentioned ϕ 50 μm Pt microdisk electrode. The Nafion coating layer was dried for 12 h at room temperature in air. The thickness of the obtained overcoat layer was estimated using a laser scanning microscope (OLS1200, Olympus) [24]. The thickness of the Nafion coating layer prepared on the Pt generator electrode was 1.3 μm.

2.2. Electrochemical measurement

The electrochemical measurements were conducted using the apparatus schematically shown in Fig. 1. Pt wire and Ag/Ag_2SO_4 [25] were utilized as the counter electrode (CE) and reference electrode (RE), respectively. All the electrode potentials in this report are referenced to the reversible hydrogen electrode potential (RHE) at the same temperature. In the SECM measurement, the above-mentioned Pt microdisk electrode and Nafion-coated Pt microdisk electrode were used as a generator. A ϕ 3 μm Pt electrode serving as a detector was attached to an arm of the SECM instrument (HV-404, Hokuto Denko). The electrode potentials of the generator and detector were controlled by a dual potentiostat (HA1010mM2B, Hokuto Denko). Prior to the SECM measurements, multiple potential cycling was conducted for cleaning the Pt surface in N_2-saturated 0.5 mol dm^{-3} H_2SO_4.

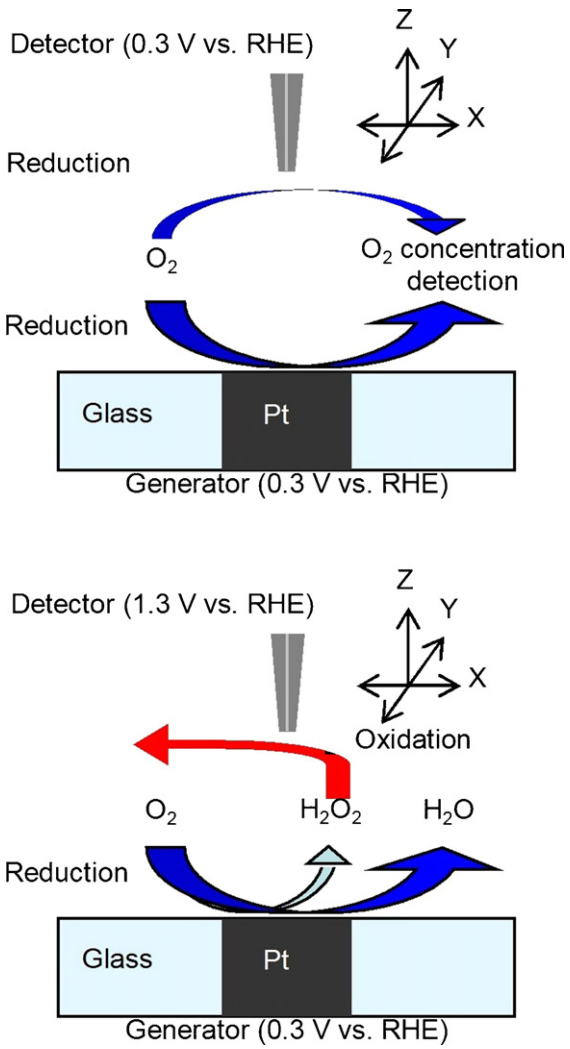

Fig. 2. Scheme of the redox competition mode (upper), the sample generation-tip collection mode (SG-TC) (lower) for the study of the ORR in 0.5 mol dm^{-3} H_2SO_4.

The SECM measurement was carried out in O_2-saturated 0.5 mol dm^{-3} H_2SO_4. An O_2 starvation for evaluating the amount of the O_2 consumption at the generator electrode was measured by the redox competition mode as shown in the upper graph of Fig. 2 [21,26]. The electrode potentials of the generator and detector were maintained at 0.3 V vs. RHE so that the O_2 reduction at the Pt definitely occurs. The position of detector was set atop of the generator at a 10 μm distance and was moved in the *X* and *Y* directions at the scan rate of 20 μm s^{-1}, as shown in Fig. 2. The central detector position on top of the generator was determined in order to observe the minimum O_2 reduction current at the detector. Subsequently, the detector was moved in the *Z* direction by an interval of 50 μm (see upper graph of Fig. 2), and again the O_2 reduction current was observed in the same manner.

The amount of H_2O_2 by-product generated during the O_2 reduction was measured in the sample generation-tip collection mode (SG-TC) as shown in the lower part of Fig. 2 [21,22,27]. The electrode potential of the detector was set at 1.3 V vs. RHE in order to detect the H_2O_2 generated during the O_2 reduction at the generator of which the potential was held at 0.3 V vs. RHE. The H_2O_2 detecting current was measured by scanning the detector in the *X*, *Y*, and *Z* directions under the same conditions as the above-mentioned O_2 starvation measurement. From the obtained results, the H_2O_2 diffusion layer thickness was estimated.

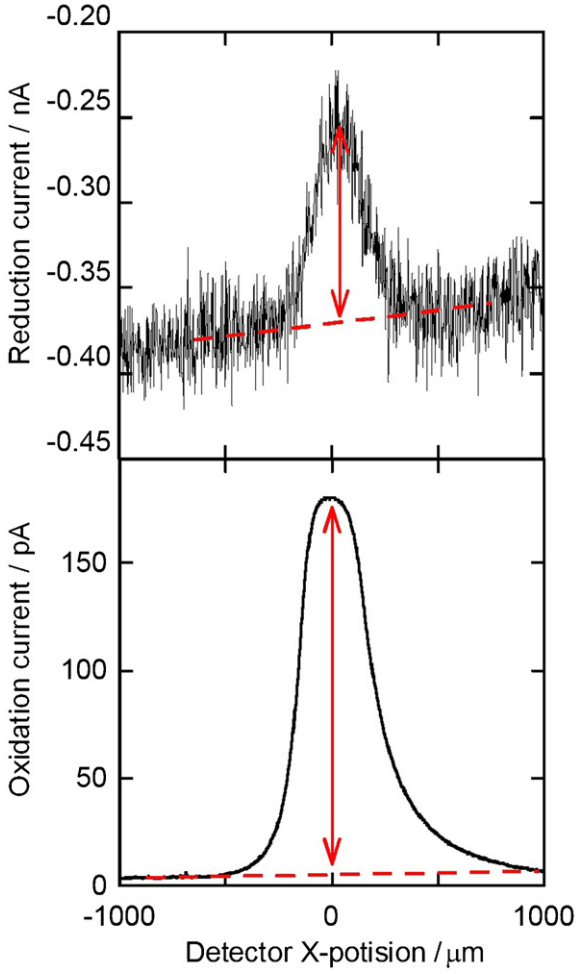

Fig. 3. Reduction current (upper) and oxidation current (lower) for detector electrode during O_2 reduction at Pt microdisk electrodes used as a generator (diameter: 300 μm, electrode potential: 0.3 V vs. RHE). The detector electrode potential was held at (a) 0.3 V vs. RHE and (b) 1.3 V vs. RHE. The generator–detector distance was 10 μm. The arrows express the maximum magnitudes of the O_2 starvation and H_2O_2 detection currents.

3. Results and discussion

3.1. O_2 starvation and H_2O_2 generation measured by scanning the detector position

The amount of the O_2 consumption at the Pt microdisk electrode as a generator was evaluated by the above-mentioned SECM technique. The principle of this measurement was evaluated in O_2-saturated 0.5 mol dm^{-3} H_2SO_4 using the ϕ 300 μm Pt microdisk electrode as a generator and the ϕ 3 μm Pt electrode as the detector. The upper graph of Fig. 3 shows the O_2 reduction current obtained at the detector vs. its X-position. During the experiment, both the generator and detector electrode potentials were held at 0.3 V vs. RHE so that the oxygen reduction simultaneously occurs. The generator–detector distance was fixed at 10 μm. From the figure, the O_2 reduction current at the detector shows a minimum at around $X = 0$ which corresponds to the central position of the generator. The decrease in the O_2 reduction current at the small detector is attributed to the O_2 consumption based on the reaction at the large-size generator.

Subsequently, only the detector electrode potential was switched to 1.3 V vs. RHE for the H_2O_2 detection. The lower graph of Fig. 3 shows the relationship between the H_2O_2 oxidation current and the X-position of the detector. In the graph, the maximum H_2O_2 oxidation current is observed at around $X = 0$.

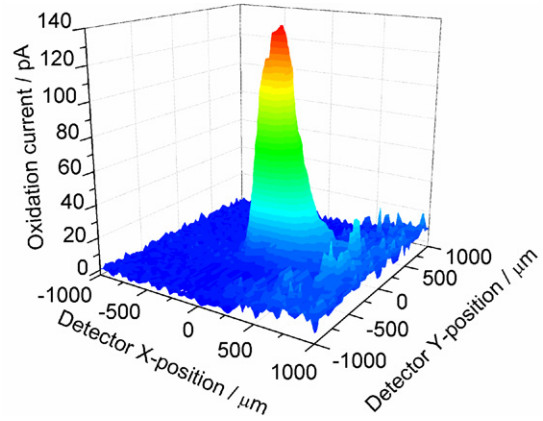

Fig. 4. Oxidation current for detector electrode scanning in X–Y plane during O_2 reduction at Pt microdisk electrode used as a generator (diameter: 300 μm, electrode potential: 0.3 V vs. RHE). The detector electrode potential was held at 1.3 V vs. RHE. The generator–detector distance was 10 μm.

Furthermore, the H_2O_2 by-product generation was investigated by scanning the X–Y-position of the detector. The scanning of the detector was conducted in an area of $\pm$1000 μm × $\pm$1000 μm. The obtained relationship between the H_2O_2 oxidation current and the X–Y plane position is shown in Fig. 4. From the figure, the maximum H_2O_2 oxidation current is observed at around $X = 0$ and $Y = 0$. At the same time, the O_2 reduction current at the detector is known to be the lowest at around $X = 0$ and $Y = 0$. Based on these results, the magnitude of the arrows shown in the upper and lower graphs of Fig. 3 are defined to be the O_2 starvation current and the H_2O_2 detection current, respectively.

3.2. Effect of generator size on the amount of O_2 consumption and H_2O_2 generation

In this section, we investigated the magnitude of the O_2 starvation and H_2O_2 detection currents by varying the generator size. The plots in the upper graph of Fig. 5 show the O_2 starvation current vs. the generator–detector distance as a function of the generator electrode diameter. From the plots of the 300 μm diameter generator, the O_2 starvation current decreased with an increase in the generator–detector distance. This result implies that O_2 can be fully supplied to the detector electrode as the influence of the O_2 consumption at the generator will be low. The same kind of relationship is seen for all the generator sizes.

Subsequently, when we compare the plots obtained at the same generator–detector distance in the upper graph of Fig. 5, the O_2 starvation current is found to be low in the order of 300 > 100 > 50 > 20 μm generator diameter. This suggests that the decrease in the generator diameter causes a decrease in the O_2 consumption at the generator. However, the O_2 starvation currents are almost the same for all the generator electrode diameters, when the generator–detector distance is greater than 110 μm. This suggests that O_2 is fully supplied to the detector electrode in the case when the generator–detector distance is greater than 110 μm.

Furthermore, the lower graph of Fig. 5 shows the H_2O_2 detection current vs. the generator–detector distance as a function of generator electrode diameter. From the plots of the 300 μm generator diameter, the H_2O_2 detection current decreases with an increase in the generator–detector distance. This implies that the generated H_2O_2 by-product diffuses not only in the detector electrode direction, but also in the X–Y direction. In other

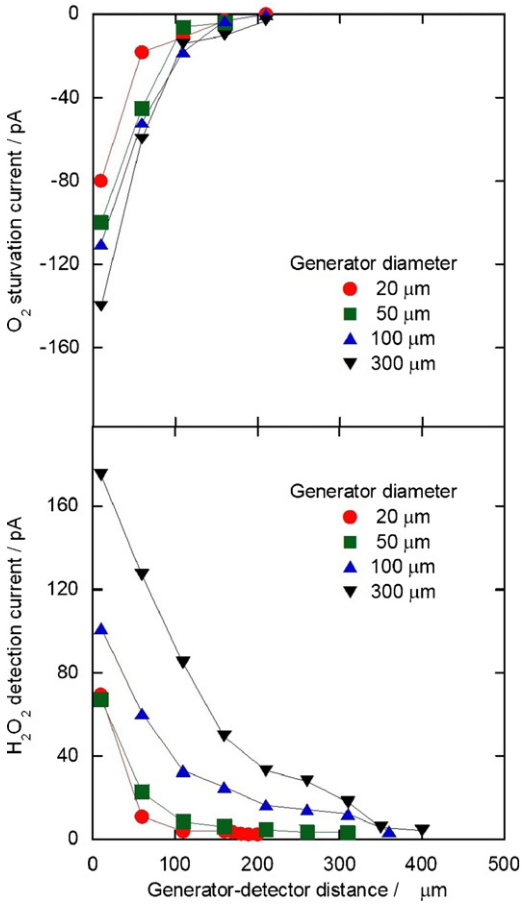

Fig. 5. O_2 starvation current (upper) and H_2O_2 detection current (lower) vs. generator–detector distance during O_2 reduction at Pt microdisk electrodes used as a generator (electrode potential: 0.3 V vs. RHE) as a function of the generator electrode diameter. The detector electrode potentials were (upper) 0.3 V vs. RHE and (lower) 1.3 V vs. RHE.

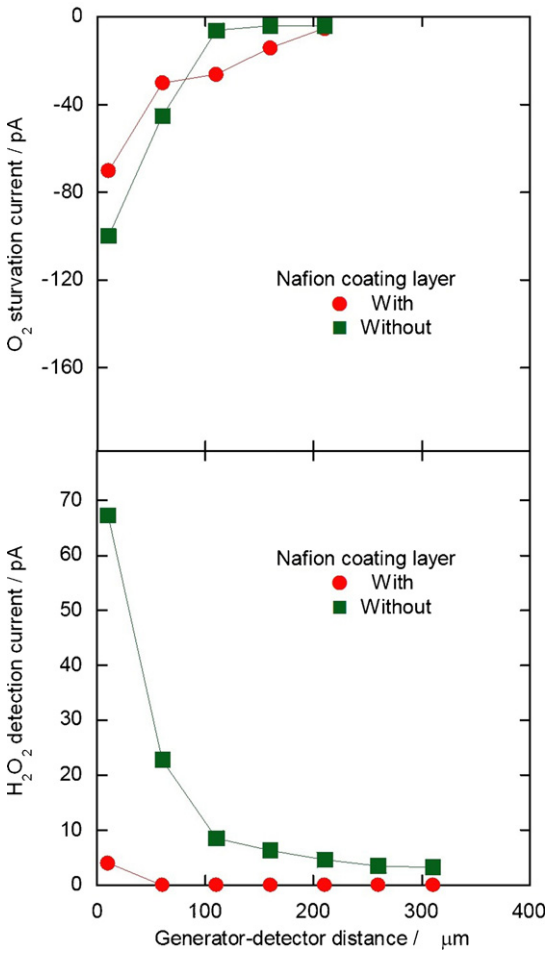

Fig. 6. O_2 starvation current (upper) and H_2O_2 detection current (lower) vs. generator–detector distance during O_2 reduction at generator (diameter: 50 μm, electrode potential: 0.3 V vs. RHE), which is Pt microdisk electrodes with (●) or without (■) Nafion coating layer. The detector electrode potentials were (upper) 0.3 V vs. RHE and (lower) 1.3 V vs. RHE.

words, the generated H_2O_2 by-product diffuses in all the directions [28]. This same kind of relationship is seen for all the generator sizes.

When the H_2O_2 detection currents are compared at the same generator–detector distance, the magnitude is in the order of 300 > 100 > 50 > 20 μm generator electrode diameter. However, the H_2O_2 detection currents for the 50 and 20 μm diameter generators are almost the same. This can be explained by the diffusion process attributed to the microelectrode characteristics [29].

When we look at the generator–detector distance when the H_2O_2 detection current is not observed, the distances are *ca.* 410, 360, 260, and 210 μm for the 300, 100, 50, and 20 μm generator diameters, respectively. This result implies that the diffusion layer thickness of H_2O_2 decreases with a decrease in the diameter size of the generator.

3.3. Amount of O_2 consumption and H_2O_2 generation at the Pt generator overcoated by a thin Nafion layer

In the PEFC cathode, the Pt/C–Nafion composite, a mixture of Pt/C and the Nafion ionomer, is used [30]. Therefore, we next investigated the amount of the H_2O_2 generation with and without a Nafion coating layer on the Pt microdisk electrode. The upper graph of Fig. 6 shows the O_2 starvation currents measured at the bare and Nafion-coated Pt microdisk electrodes by changing the generator–detector distance. Based on this result, the O_2 starvation currents are not significantly changed by coating the Nafion layer on the Pt, which means that the amounts of the O_2 consumption at the two electrodes are almost the same.

Subsequently, the H_2O_2 detection current was measured in the same manner. The lower graph of Fig. 6 shows H_2O_2 detection current vs. the generator–detector distance between the two electrodes. The H_2O_2 detection current from the Nafion-coated Pt electrode was dramatically suppressed when compared to that from the bare Pt electrode. Furthermore, the thicknesses of the H_2O_2 diffusion layer are estimated to be *ca.* 260 and 60 μm for the bare and Nafion-coated electrodes, respectively. The diffusion layer thickness of H_2O_2 is significantly reduced by the Nafion overcoat.

Based on the above result, the amounts of the O_2 consumption are not significantly changed by the existence of the Nafion overcoat. Therefore, the amount of the H_2O_2 by-product generation will not be significantly changed at the two electrodes. However, a big difference is observed for the H_2O_2 diffusion layer by the Nafion coating. The following two reasons are considered to explain the result. One is caused by the small diffusion coefficient of H_2O_2 in the Nafion. The other possible factor is based on the low desorption rate of H_2O_2 from the Pt surface by the presence of Nafion. It is well known that the H_2O_2 by-product is generated at the cathode in the practical PEFC operation [31,32]. In order to suppress the amount of generated H_2O_2, it will be an effective method to cover the Pt surface by the Nafion layer. In the future, we have a plan to dis-

close the suppression phenomenon by varying the thickness of the Nafion coating layer.

4. Conclusions

We measured the amount of generated H_2O_2 during O_2 reduction at a Pt generator of the SECM, and then an estimation method of the H_2O_2 diffusion layer thickness was established. The obtained results are summarized as follows.

(1) A significant amount of O_2 consumption and generated H_2O_2 are detected at the center of each generator electrode. Therefore, the O_2 starvation and H_2O_2 detection currents are defined by the detector current measured at this position.
(2) The amount of O_2 consumption and generated H_2O_2 are found to decrease when the generator electrode diameter becomes small. Also, the thicknesses of the diffusion layer of H_2O_2 decrease with a decrease in the diameter of the Pt generator. The H_2O_2 diffusion process is found to change when the generator diameter is less than 50 μm.
(3) The Nafion layer prepared on the Pt electrode suppresses the amount of H_2O_2 diffusion whereas the O_2 consumption is not suppressed.

Acknowledgement

The present work was financially supported by the Research and Development of Polymer Electrolyte Fuel Cells Project from the New Energy and Industrial Technology Development Organization (NEDO), Japan.

References

[1] G. Hoogers, Fuel Cell Technology Handbook, CRC Press, United Kingdom, 2003 (section 6).
[2] K. Kinoshita, Electrochemical Oxygen Technology, John Wiley & Sons, Inc, New York, 1992 (section 4).
[3] G. Hoogers, Fuel Cell Technology Handbook, CRC Press, United Kingdom, 2003 (section 2).
[4] M. Inaba, H. Yamada, J. Tokunaga, A. Tasaka, Electrochem. Solid-State Lett. 7 (2004) A474–A476.
[5] F. Dundar, A. Smirnova1, X. Dong, A. Ata, N.J. Sammes, Fuel Cell Sci. Technol. 3 (2006) 428–433.
[6] M.M. Markovic, P.N. Ross Jr., Surf. Sci. Rep. 45 (2002) 117–229.
[7] N. Ramaswamy, N. Hakim, S. Mukerjee, Electrochim. Acta 53 (2008) 3279–3295.
[8] T. Kinumoto, M. Inaba, Y. Nakayama, K. Ogata, R. Umebayashi, A. Tasaka, Y. Iriyama, T. Abe, Z. Ogumi, J. Power Sources 158 (2006) 1222–1228.
[9] E. Endoh, S. Hommura, in: F.N. Büchi, M. Inaba, T.J. Schmidt (Eds.), Polymer Electrolyte Fuel Cell Durability, Springer, New York, 2009, pp. 119–132.
[10] A. Pozio, R.F. Silva, M.D. Francesco, L. Giorgi, Electrochim. Acta 48 (2003) 1543–1549.
[11] M. Umeda, T. Maruta, M. Inoue, A. Nakazawa, J. Phys. Chem. C 112 (2008) 18098–18103.
[12] M. Watanabe, H. Igarashi, K. Yosioka, Electrochim. Acta 40 (1995) 329–334.
[13] A. Ayad, Y. Naimi, J. Bouet, F. Fauvarque, J. Power Sources 130 (2004) 50–55.
[14] A. Ignaszak, S. Ye, E. Gyenge, J. Phys. Chem. C 113 (2009) 298–307.
[15] M.Y. Shen, S.P. Chiao, D.S. Tsai, D.P. Wilkinson, J.C. Jiang, J. Electrochim. Acta 54 (2009) 4297–4304.
[16] V. Stamenković, T.J. Schmidt, P.N. Ross, N.M. Marković, J. Electroanal. Chem. 554 (2003) 191–199.
[17] C. Coutanceau, M.J. Croissant, T. Napporn, C. Lamy, Electrochim. Acta 46 (2000) 579–588.
[18] N. Wakabayashi, M. Takeichi, H. Uchida, M. Watanabe, J. Phys. Chem. B 109 (2005) 5836–5841.
[19] H. Yano, E. Higuchi, H. Uchida, M. Watanabe, J. Phys. Chem. B 110 (2006) 16544–16549.
[20] M. Itagaki, Y. Fujimura, I. Shitanda, K. Watanabe, T. Hachiya, Anal. Sci. 22 (2006) 1315–1318.
[21] K. Eckhard, W. Schuhmann, Electrochim. Acta 53 (2007) 1164–1169.
[22] C.M. Sánchez-Sánchez, J. Rodríguez-López, A.J. Bard, Anal. Chem. 80 (2008) 3254–3260.
[23] M. Umeda, M. Mohamedi, I. Uchida, Langmuir 17 (2001) 7970–7972.
[24] K. Kashima, M. Umeda, A. Yamada, Bunnseki Kagaku 53 (2004) 1055–1059 (in Japanese).
[25] M. Umeda, Y. Kuwahara, A. Nakazawa, M. Inoue, J. Phys. Chem. C 113 (2009) 15707–15713.
[26] A.O. Okunola, T.C. Nagaiah, X. Chen, K. Eckhard, W. Schuhmann, M. Bron, Electrochim. Acta 54 (2009) 4971–4978.
[27] A.R. Kucernak, P.B. Chowdhury, C.P. Wilde, G.H. Kelsall, Y.Y. Zhu, D.E. Williams, Electrochim. Acta 45 (2000) 4483–4491.
[28] A.J. Bard, L.R. Faulkner, Electrochemical Methods, John Wiley & Sons, Inc, New York, 1980 (section 4).
[29] C.G. Zoski, Handbook of Electrochemistry, Elsevier, oxford, 2007 (section 6).
[30] G. Sasikumar, J.W. Ihm, H. Ryu, J. Power Sources 132 (2004) 11–17.
[31] Q. Guo, P.N. Pintauro, H. Tang, S. O'Connora, J. Membr. Sci. 154 (1999) 175–181.
[32] M. Inaba, T. Kinumoto, M. Kiriake, R. Umebayashi, A. Tasaka, Z. Ogumi, Electrochim. Acta 51 (2006) 5746–5753.